

Temperature dependence of spin-torque-driven self-oscillations

M. L. Schneider,¹ W. H. Rippard,² M. R. Pufall,² T. Cecil,² T. J. Silva,² and S. E. Russek²

¹*Department of Physics and Astronomy, University of Montana, Missoula, Montana 59812, USA*

²*Electromagnetics Division, National Institute of Standards and Technology, Boulder, Colorado 80305, USA*

(Received 21 July 2009; revised manuscript received 10 September 2009; published 15 October 2009)

We have measured the temperature dependence of spin-torque-driven self-oscillations in point-contact nano-oscillators for both in-plane and out-of-plane applied fields. We find that the linewidth for both field geometries is qualitatively similar. In the absence of observable low-frequency noise, at high temperatures the linewidth decreases roughly linearly as the temperature decreases. However, extrapolation of the quasilinear region to a zero-temperature linewidth intercept can yield either a positive or negative value. This variation in the zero-temperature linewidth intercept indicates that a range of mechanisms must be involved in setting the linewidth. When $1/f$ noise is present in the device power spectrum, the linewidth varies quasiexponentially with temperature. While the linewidth versus temperature behavior is similar for both in-plane and out-of-plane applied fields, their output power versus current variation with temperature is qualitatively different.

DOI: [10.1103/PhysRevB.80.144412](https://doi.org/10.1103/PhysRevB.80.144412)

PACS number(s): 75.75.+a, 76.50.+g, 72.25.-b

I. INTRODUCTION

The spin-transfer effect is known to give rise to microwave dynamics in a variety of magnetic nanostructures and magnetic materials¹⁻³ with the two most common geometries being nanopillar and point-contact devices. Both geometries confine a spin-polarized current within a diameter on the order of 100 nm so that the required high current densities can be obtained. In the nanopillar geometry the magnetic volume undergoing precession is lithographically patterned and, in the simplest case, is independent of the strength and orientation of the applied magnetic field. Other groups have investigated the role of temperature in determining the linewidth of nanopillar devices for in-plane applied fields and have found results consistent with the linewidth being determined by phase fluctuations and two-state switching.^{4,5} In the nanocontact geometry a nanoscale electrical contact is made to a macroscopic magnetic film, and the magnetic region undergoing precession can be either localized under the contact or extended, depending on the orientation and strength of the applied magnetic field.^{6,7} One potential advantage of the nanocontact geometry is that the fabrication process does not result in the formation of ferromagnetic oxides in the active device area, which have been shown to play a complicating role in magnetization damping and dynamics at low temperatures.⁸ We investigate thermal contributions that limit the linewidth of spin-transfer excitations in nanocontact devices and compare the results to recent theoretical efforts.⁹⁻¹¹

II. EXPERIMENT

The nanocontact devices discussed here consist of a 60 nm nominal diameter electrical contact made to the top of a continuous $10\ \mu\text{m} \times 20\ \mu\text{m}$ spin-valve mesa¹² of composition Ta(3 nm)/Cu(15 nm)/Co₉₀Fe₁₀(20 nm)/Cu(4 nm)/Ni₈₀Fe₂₀(5 nm)/Cu(3 nm)/Ta(3 nm). Precessional motion is induced in the NiFe layer through the spin-transfer effect and the high-moment CoFe layer acts as the fixed layer. Precessional motion of the free layer results in a

time-varying resistance via the giant magnetoresistance effect. Since the device is dc biased, this produces a microwave voltage that is measured with a spectrum analyzer. For these studies, the devices are mounted in a variable temperature (5–350 K) He gas bath cryostat, where magnetic fields up to $\mu_0 H = 600$ mT can be applied at any angle to the film plane. The quoted temperatures below are those of the He bath and not those of the samples, which are expected to be a few tens of kelvins higher due to ohmic heating.¹³ Data shown here are from a few devices but the qualitative features discussed have been measured in tens of devices in each of the applied field geometries.

III. IN-PLANE APPLIED FIELDS

Figure 1 shows a typical spectral output as a function of dc taken at $T = 40$ K and $\mu_0 H = 32.5$ mT. The field was applied in the plane of the film and parallel to the anisotropy

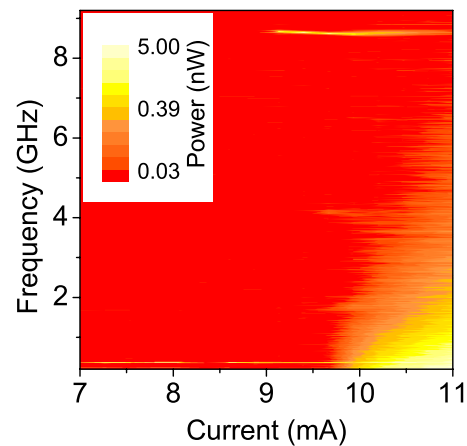


FIG. 1. (Color online) Two-dimensional plot showing the spectral output as a function of bias current for a device under in-plane applied field of $\mu_0 H = 32.5$ mT. The power spectral density is shown in a log color scale 0–5 nW. The onset current is roughly 9 mA and the $1/f$ signal appears at 10 mA. These data were taken at a bath temperature of 40 K.

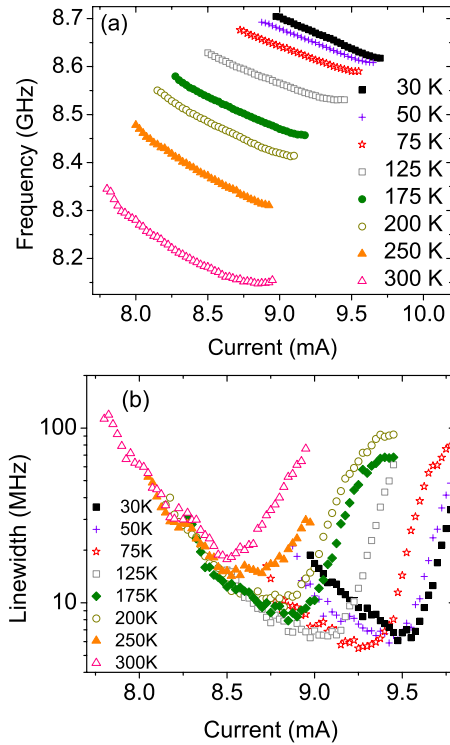


FIG. 2. (Color online) (a) Oscillation frequency as a function of applied dc for a number of different temperatures. (b) Linewidths (full width at half maximum as determined by Lorentzian fits to the data) for the corresponding data in part (a), shown on a semilog scale. The error bars from the fits [for both (a) and (b)] are smaller than the data points and so are not visible. These data were taken with an applied field of $\mu_0 H = 50.0$ mT

axis. For currents just above the onset of precession, in this case at 9 mA, the spectral output from the device consists of a large peak near $f = 8.7$ GHz. Although not clearly visible, there is also a much smaller signal at half of this frequency. Using the Kittel equation for the ferromagnetic resonance (FMR) for this field geometry, we identify the signal at 8.7 GHz as the second harmonic of the quasiuniform FMR mode.¹⁴ The relative strength of the first and second harmonics indicates that the precession axis of the free layer is almost parallel to the direction of the fixed layer.¹² At higher current values, the power in the second harmonic mode decreases and a significant low-frequency component appears, indicating the onset of a random telegraph process in which the system toggles between states with different resistance values.^{15,16} The low-frequency component results from a current-induced noise process and gives rise to power spectra analogous to $1/f$ noise, although in the functional form the noise follows may not precisely be $1/f$.

In Fig. 2 we examine the behavior of the second harmonic of the same device taken with an applied field of $\mu_0 H = 50$ mT. With this applied field the bias current must be increased further above the onset current before the low-frequency noise can be observed. The data in Fig. 2(a) show the current dependence of the self-oscillation frequency as determined by Lorentzian fits for several temperatures. At a given temperature the frequency of the peak decreases with increasing current, which results from the current depen-

dence of the oscillation trajectory.¹² This leads to the excitation being localized underneath the contact area once the mode frequency is less than the FMR frequency.^{6,7} As the temperature is decreased, several of the oscillator characteristics change, e.g., the oscillation frequencies and critical currents increase. These changes reflect the temperature dependence of the magnetic parameters in the device such as the saturation magnetization M_s , effective anisotropies, and current polarization. Without the presence of an oxide we expect M_s and the effective anisotropies to vary by about 10% while the current polarization may vary by about 50%.¹⁷ Figure 2(b) shows the corresponding linewidth Δf vs current at the same temperatures. We use the full width at half maximum as the value of our linewidth throughout this paper. At a given temperature, the linewidth generally decreases with increasing current to a minimum value and then increases. The initial decrease in the linewidth with current can be explained as resulting from both the damping torque and spin torque being smallest at onset and then increasing with current, resulting in a precession, that is, more susceptible to thermal fluctuations near onset.⁶ The linewidth increase at larger currents correlates with the onset of low-frequency $1/f$ noise in the power spectrum, which can be explained by a stochastic switching processes.^{15,16} These two behaviors reflect two distinct linewidth broadening mechanisms and their temperature dependencies will be discussed separately. We will start by analyzing the low current data that were obtained in the absence of any obvious $1/f$ noise. We presume that the linewidth in this regime is dominated by thermal magnetic fluctuations giving rise to phase noise in the excited mode, which has been shown to be the case for similar dynamics in these devices at room temperature.¹⁸ The strong current dependence of the linewidth and the temperature dependencies of the materials properties of the device complicate the analysis of the temperature dependence of the oscillation linewidths. Considering the behavior in terms of a macrospin approximation, one would like to determine the thermal contributions to oscillator linewidth by directly comparing Δf of a *specific trajectory* (magnetization orbit) at discrete temperatures. However, because of the changing materials properties, this cannot be accomplished by simply comparing the linewidths at a fixed frequency, fixed current, or fixed power output over the entire temperature range. For example, in Fig. 2 there is no single current or frequency at which the device exhibits oscillations for all temperatures, and the critical current I_c for the onset of precession also varies with temperature.

In Fig. 3 we show the linewidth as a function of temperature for two different in-plane field values. The data in Fig. 3(a) are the linewidth near onset and at the minimum obtained with an applied field of $\mu_0 H = 50$ mT. These data have been extracted from the data shown in Fig. 2(b). The behavior of both the onset and the minimum of the linewidth follow the same trends with only a scaling difference. Between 350 and roughly 150 K, both the minimum and the onset linewidth vary approximately linearly with temperature. At lower temperatures both the linewidths effectively saturate. This behavior is commonly seen, occurring in a majority of the measured devices. Depending on the applied field strength and orientation, the linewidth saturation tem-

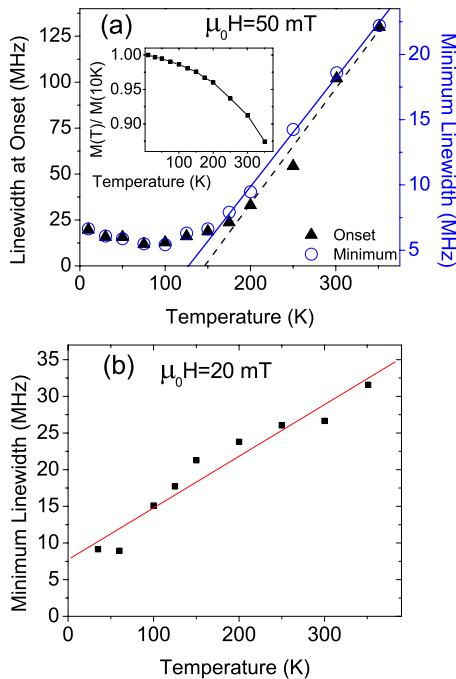


FIG. 3. (Color online) (a) Linewidths near onset (closed triangles) and near the minimum (open circles) for the data in Fig. 2(b). The data represent the average values for the first five data points after onset and the five data points centered on the minimum. The dashed and solid lines are fits (for $T > 150$ K) to the near onset and minimum linewidths, respectively. (Inset) The relative effective magnetization of the region undergoing oscillations, as determined through the Kittel relation, as a function of temperature. (b) Linewidth data (closed squares) near the onset for an in-plane applied field of $\mu_0 H = 20$ mT as a function of temperature. The line is a fit of the data between 10 and 350 K and has a positive intercept. The error bars from the fits [for both (a) and (b)] are smaller than the data points.

perature of a particular device can vary between roughly 50 and 150 K, and the linewidth at saturation varies between a megahertz and a few tens of megahertz. While the linewidths are consistent between runs on the same samples, we do not find a robust dependence of the linewidth value as a function of in-plane applied field. We believe that this is likely due to changes in the particular mode being observed that can result from changes in the applied field. Several aspects of the data suggest that the linewidth saturation is *not* due simply to a saturation of the effective temperature of the device as a result of ohmic heating. First, the resistance of the device continues to decrease and the onset current continues to increase over the entire temperature range. Additionally, the oscillation frequency of the device [see Fig. 2(a)] does not saturate with decreasing temperature in the same manner as the linewidth does. In the inset in Fig. 3(a), we use the Kittel equation to calculate the relative saturation magnetization based upon the onset frequency at each temperature. This indicates that the effective magnetization of the region undergoing precession does not saturate as the bath temperature drops below 150 K.

We examine the linewidth above the saturation temperature in Fig. 3(a). Linear fits to the data at the onset and at the

minimum for $T > 150$ K yield $T=0$ intercepts of -90 ± 10 and -7 ± 1 MHz, respectively. In other words, the data in Fig. 3(a) have intercepts at $T=0$ K that are negative to within the accuracy of the measurement. The linear temperature dependence is consistent with models for thermally driven phase noise, such as those of Kim *et al.*,⁹ which also predicts that linewidth should approach zero in a linear fashion as the temperature goes to zero kelvin. Hence, the data overall are not consistent with the present theories that describe the linewidth as being limited by phase noise.

In Ref. 5, the authors attributed qualitatively similar behavior to the onset of two-state fluctuations in their nanopillar devices. In the case that two-state fluctuations are responsible for the measured oscillation linewidths, the relationship of Δf vs T should be exponential with $\Delta f - \Delta f_0 \propto (e^{-E_b/k_B T})$, where E_b is the energy barrier between the states and k_B is Boltzmann's constant.⁵ However, there is no measurable $1/f$ noise for the data in Fig. 3(a), implying that for the two-state model to be valid, both states would have to have nearly identical resistances. Beyond this, the variation in Δf is too small over the accessible temperature range, less than an order of magnitude, to be able to discern the difference between a linear and exponential fit. Furthermore, no model exists for the two states themselves, making a comparison with a fluctuating two-state system difficult. Thus while a linear fit to an exponentially varying data set will generally yield a negative intercept, and could explain the data, a detailed comparison with such a model does not yield additional insight in our case.

Figure 3(b) shows the linewidth versus temperature data taken on the same device and geometry, but with a different applied field. For this particular device and geometry, when the applied in-plane field is changed to $\mu_0 H = 20$ mT, there is a different response of the linewidth as a function of temperature. These data were taken at the linewidth minimum. As with the previous data, the linewidth here varies roughly linearly with temperature. However, the linear dependence occurs over the entire temperature range and has a positive zero-temperature intercept of 8 ± 1 MHz. In the absence of other broadening mechanisms, if a spin torque oscillator incurring thermal perturbations exhibits a restoring torque that is linearly proportional to the perturbation amplitude, the resulting linewidth is dominated by the induced phase noise, and is linear in temperature with a $T=0$ intercept of 0 MHz.⁹ We will refer to this mechanism of broadening as thermally driven phase noise. Thus, these data are consistent with a model that has a linear restoring torque along with an additional temperature-independent broadening mechanism. As demonstrated by the above data, in general one can find cases where the linear region in the linewidth versus temperature of the data has a negative intercept or a positive intercept by varying applied field and geometry.

An important point evident from the data presented above is that the functional form of the temperature dependence of the measured linewidth, e.g., a linear dependence, is insufficient to determine the responsible broadening mechanism. While all of the data presented above have nominally linear dependences of linewidth at higher temperature, their intercepts suggest different broadening mechanisms are present. For instance, the intercept of the data in Fig. 3(b) is consis-

tent with thermally driven phase noise dominating the measured linewidth except at the lowest temperatures. On the other hand, the negative intercept of the data in Fig. 3(a) suggests that a different mechanism is responsible. Hence, we conclude that the $T=0$ K intercept of Δf vs T data should be examined in assessing models or theories of the linewidth mechanisms present in spin-transfer oscillators.

IV. OUT-OF-PLANE FIELDS

We have also measured the behavior of spin-torque oscillators for out-of-plane applied magnetic fields. As discussed above, when comparing the temperature dependence of the oscillation linewidths, the comparison needs to be done for magnetization trajectories that are similar over the entire temperature range. This can be even more challenging in the out-of-plane geometry because changes in M_s with temperature will tend to alter the equilibrium configuration of the spin valve, leading to excitation trajectories that can change significantly over the measurement temperatures, depending on the applied field strength and orientation. For instance, we have found that when we apply fields $\mu_0 H < 600$ mT at a canted angle with respect to the film plane, the reorientation of the magnetization is enough to give complicated (non-monotonic) temperature-dependent linewidths even when analyzing the data at onset, or at the linewidth minimum. This is accompanied by significant changes in f vs I and df/dI vs I with T , indicating that the magnetization trajectories are changing significantly and thus cannot be directly compared.

We compensate for the reorientation effect of the free layer in the out-of-plane geometry by applying the largest field possible ($\mu_0 H = 600$ mT in our system) nominally perpendicular to the film plane. In this geometry the excitations have similar f vs I and df/dI vs I behaviors over the measured temperature range. Consequently, these measurements describe similar orbits and so can be meaningfully compared to each other as a function of temperature.

The data in Fig. 4 were taken with $\mu_0 H = 600$ mT applied nominally perpendicular to the film plane. Assuming that the demagnetization field is approximately M_s , this rotates the magnetization of the NiFe layer out of the film plane by approximately 30° . Figure 4(a) shows the oscillation frequency as a function of dc bias current for temperatures ranging from 65 to 350 K. The data show a frequency increase with increasing current in this geometry. Since the precession frequency is above the FMR frequency, theory suggests that this results in a nonlocalized excitation with spin waves being radiated into the surrounding film.¹⁹ This differs from the in-plane case where the excitation is presumably localized to a small volume directly underneath the contact.^{6,7}

Figure 4(b) shows the temperature dependence of the linewidth at onset. Similar to the in-plane geometry, we find that the linewidth scales roughly linearly with temperature at high temperatures in the out-of-plane geometry with a low-temperature saturation of the linewidth. In this particular data set, a linear fit of the data above 100 K gives a $T=0$ K intercept of 1 ± 0.5 MHz. These data are nominally consis-

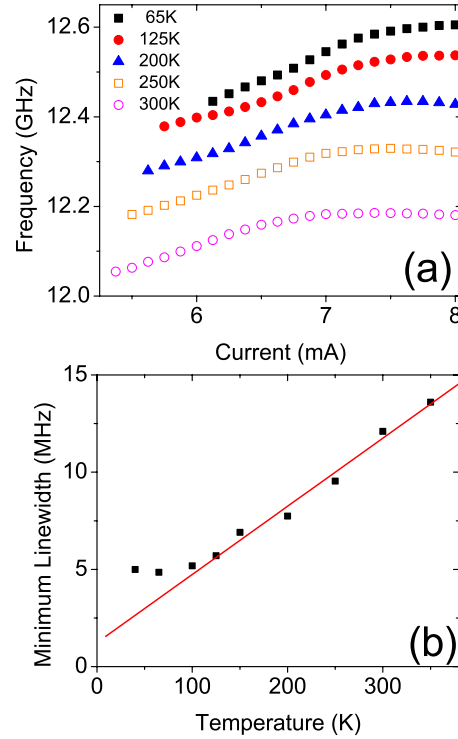


FIG. 4. (Color online) (a) Oscillation frequency as a function of applied dc for a number of different temperatures with an out-of-plane applied field of $\mu_0 H = 600$ mT. (b) The corresponding linewidth as a function of temperature averaged at ± 0.25 mA about the local minimum near the onset current. The error bars from the fits [for both (a) and (b)] are smaller than the data points and so are not visible.

tent with models where the dominant broadening mechanism is thermally driven phase noise.⁹ In general, we do not see a difference in the behavior of the linewidth vs temperature between the in-plane and out-of-plane applied field geometries. Thus, generally for out-of-plane applied fields, the extrapolation of the linear Δf vs T region gives linewidths with either positive or negative intercepts, depending on the device under study and small changes in applied field or geometry. Similar to the case of an in-plane applied field, this suggests either that other sources of noise are adding to the linewidth, or that the device is being driven into a regime where the restoration torque is nonlinear. These results have been measured in tens of devices for the two different geometries (in plane and out of plane) and indicate that the general trends reported here (at higher temperatures the dependence of the linewidth on temperature is nominally linear with a potential low-temperature saturation of the linewidth) are robust with respect to sample-to-sample variations and the exact magnetic configuration under consideration.

V. Δf VS T IN THE PRESENCE OF $1/f$ Noise

The data and analysis presented above are limited to situations in which the device is undergoing steady-state oscillations in the absence of $1/f$ noise. For comparison, in Fig. 5 we show the temperature-dependent behavior of a device

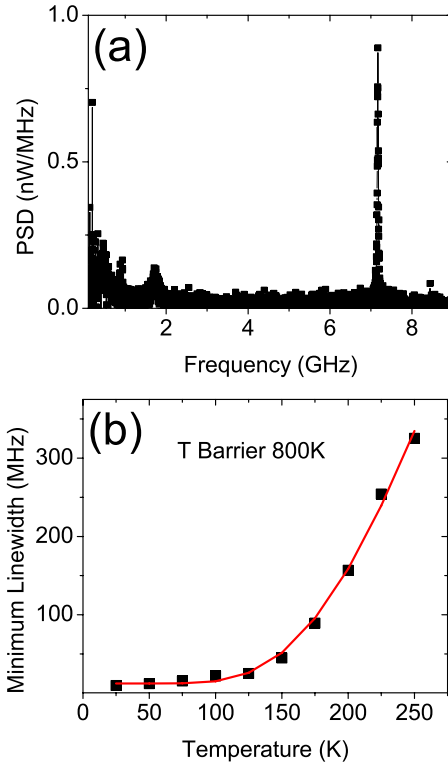


FIG. 5. (Color online) (a) Spectral trace showing the coexistence of an oscillating state and $1/f$ noise indicating the presence of two-state switching. The data were taken in an applied field of 450 mT at an angle of about 90° with respect to the film plane. (b) Average linewidth of the high-frequency peak for the first five data points after $1/f$ noise is first measurable. The error bars from the fits are smaller than the data points.

with an out-of-plane applied field showing significant $1/f$ noise, which is indicative of fluctuations into and out of the precessional state.^{15,20} Figure 5(a) is a power spectrum from a device showing a high-frequency peak at 7.2 GHz along with a $1/f$ signal at low frequencies. The additional small peak around 1.7 GHz is the result of an external noise source, which is independent of the device, applied field, or geometry but is not perfectly subtracted from the experimental spectra. Since no secondary spectral peak from the device is observed, it is presumably switching between an oscillating state and a quiescent one. Figure 5(b) shows the linewidth of the high-frequency peak, as determined by averaging the linewidth data for the first 0.5 mA data points above the current at which point the $1/f$ noise is apparent. We see that the linewidth depends much more strongly on temperature in the presence of $1/f$ noise: The linewidth varies by a factor 30 over the measured temperature range when the oscillator emits $1/f$ noise, whereas the linewidth varies by less than a factor of 10 in the absence of any measurable low frequency noise (see Figs. 3 and 4). A fit of a two-state model (see Sec. III) to the data is also shown in Fig. 5(b). From the fit we find an energy barrier of approximately 800 K, nominally in agreement with previous findings.^{5,15}

VI. DEPENDENCE OF OSCILLATION POWER ON T

In contrast to the qualitatively similar dependence of the oscillation linewidths on temperature for the two applied

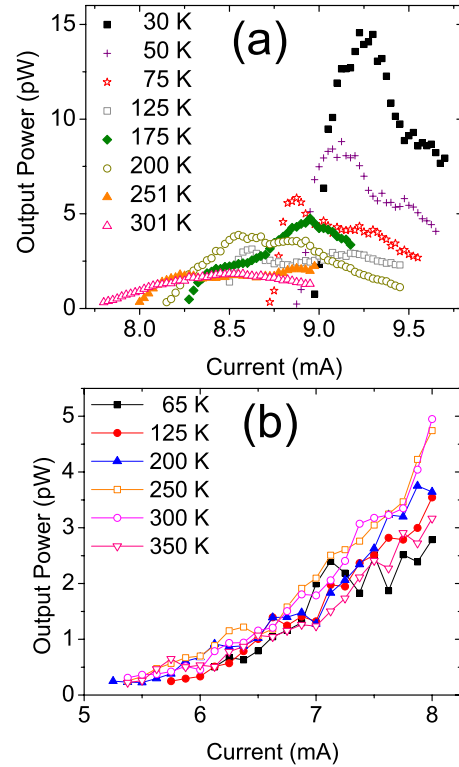


FIG. 6. (Color online) [(a) and (b)] Measured device output power as a function of current for a number of different temperatures corresponding to the data shown in Figs. 2 and 4, respectively. The power corresponds to the integrated area under the spectral peak. The gain of the amplifier has been divided out. However, the impedance mismatch between the $\approx 10 \Omega$ device and 50Ω spectrum analyzer has not been taken into account nor has the attenuation of the signal from the wire bonds.

field geometries, the temperature dependence of their output powers, the integrated Lorentzian peaks, are distinctly different. In Figs. 6(a) and 6(b), we show the device output powers corresponding to the data shown in Figs. 2 and 4, respectively. Figure 6(a) shows output power versus current for several temperatures for in-plane fields. The slope of the initial increase in output power versus current increases from roughly 3 pW/mA at 300 K to 90 pW/mA at 30 K. This is consistent with a strongly thermally activated process, as is discussed in Ref. 21. For out-of-plane fields [Fig. 6(b)], the slope of output power vs applied current is effectively independent of temperature, with the slope of the onset power changing by only about 40% over the measured temperature range. The different behavior for the two geometries is consistent with the fact that for parallel alignment between the fixed and free layers, the absolute value of the spin torque at onset is small and susceptible to thermal agitation. In the out-of-plane geometry the misalignment of the layers results in a finite spin torque at onset and is less dependent on thermal agitation for the onset of steady-state oscillations. In addition, the differences in the power behavior between the two geometries might arise from the change in the spin-wave mode between localized spin waves for the in-plane precession and propagating for the out-of-plane precession. Despite the difference in the temperature dependence of the rate of

power increase at the onset for in-plane and out-of-plane oscillations, a corresponding difference in the temperature dependence of their linewidths is *not* observed.

It should be noted that there is attenuation in the system that varies between roughly 1 and 2 dB/GHz, depending on the integrity of the short wire bond connections made to the device and the cabling, which is difficult to precisely calibrate. Thus, a direct comparison of the output power between the two geometries is not possible because of the change in oscillator frequency between the two geometries. However, this does not affect the comparison of the output power versus temperature for a particular device. Further, this does not play a role in the different behaviors that we observe in the two geometries.

VII. CONCLUSION

We have measured the temperature dependence of the linewidth and power output of spin-torque-driven self-oscillations in point contact nano-oscillators in two different applied field geometries. In the presence of $1/f$ noise, the change in linewidth can be a factor of 30 from 350 to 50 K. This is in contrast to the quasilinear behavior where the change in linewidth over the same temperature span is about

a factor of 5. For both in-plane and out-of-plane geometries, in the absence of measurable two-state switching ($1/f$ noise), the linewidth varies roughly linearly with temperature, with a possible low-temperature saturation point. Extrapolation of the quasilinear region to zero temperature can yield either positive, negative, or near zero intercept values. We have not found a systematic variation that leads to a consistent positive or negative intercept value. A zero intercept linewidth is expected if the dominant broadening mechanism is thermally driven phase noise. A positive intercept is consistent with thermally driven phase noise in the presence of an additional temperature-independent broadening mechanism. However, the presence of negative intercept values for some data suggests that the dominant broadening mechanism is not always thermally driven phase noise, even when the variation in the linewidth with temperature is linear near room temperature. In addition, while the behavior of the linewidth in the in-plane and out-of-plane geometries is qualitatively the same, the behavior of the output power versus temperature is qualitatively different between the two geometries.

ACKNOWLEDGMENT

This work was supported in part by the NIST Office of Microelectronics Programs.

-
- ¹M. R. Pufall, W. H. Rippard, and T. J. Silva, *Appl. Phys. Lett.* **83**, 323 (2003).
- ²M. D. Stiles and J. Miltat, in *Spin Dynamics in Confined Magnetic Structures III*, edited by B. Hillebrands and A. Thiaville (Springer, Berlin, 2006).
- ³K. Yagami, A. A. Tulapurkar, A. Fukushima, and Y. Suzuki, *Appl. Phys. Lett.* **85**, 5634 (2004).
- ⁴Q. Mistral, J. V. Kim, T. Devolder, P. Crozat, C. Chappert, J. A. Katine, M. J. Carey, and K. Ito, *Appl. Phys. Lett.* **88**, 192507 (2006).
- ⁵J. C. Sankey, I. N. Krivorotov, S. I. Kiselev, P. M. Braganca, N. C. Emley, R. A. Buhrman, and D. C. Ralph, *Phys. Rev. B* **72**, 224427 (2005).
- ⁶G. Consolo, B. Azzerboni, L. Lopez-Diaz, G. Gerhart, E. Bankowski, V. Tiberkevich, and A. N. Slavin, *Phys. Rev. B* **78**, 014420 (2008).
- ⁷S. E. Russek, S. Kaka, W. H. Rippard, M. R. Pufall, and T. J. Silva, *Phys. Rev. B* **71**, 104425 (2005).
- ⁸N. C. Emley, I. N. Krivorotov, O. Ozatay, A. G. F. Garcia, J. C. Sankey, D. C. Ralph, and R. A. Buhrman, *Phys. Rev. Lett.* **96**, 247204 (2006).
- ⁹J. V. Kim, Q. Mistral, C. Chappert, V. S. Tiberkevich, and A. N. Slavin, *Phys. Rev. Lett.* **100**, 167201 (2008).
- ¹⁰J. V. Kim, V. Tiberkevich, and A. N. Slavin, *Phys. Rev. Lett.* **100**, 017207 (2008).
- ¹¹V. S. Tiberkevich, A. N. Slavin, and J. V. Kim, *Phys. Rev. B* **78**, 092401 (2008).
- ¹²W. H. Rippard, M. R. Pufall, S. Kaka, S. E. Russek, and T. J. Silva, *Phys. Rev. Lett.* **92**, 027201 (2004).
- ¹³I. N. Krivorotov, N. C. Emley, A. G. F. Garcia, J. C. Sankey, S. I. Kiselev, D. C. Ralph, and R. A. Buhrman, *Phys. Rev. Lett.* **93**, 166603 (2004).
- ¹⁴C. Kittel, *Phys. Rev.* **73**, 155 (1948).
- ¹⁵M. R. Pufall, W. H. Rippard, S. Kaka, S. E. Russek, T. J. Silva, J. Katine, and M. Carey, *Phys. Rev. B* **69**, 214409 (2004).
- ¹⁶S. Urzhudin, N. O. Birge, W. P. Pratt, and J. Bass, *Phys. Rev. Lett.* **91**, 146803 (2003).
- ¹⁷M. L. Schneider, M. R. Pufall, W. H. Rippard, S. E. Russek, and J. A. Katine, *Appl. Phys. Lett.* **90**, 092504 (2007).
- ¹⁸M. W. Keller, A. B. Kos, T. J. Silva, W. H. Rippard, and M. R. Pufall, *Appl. Phys. Lett.* **94**, 193105 (2009).
- ¹⁹M. R. Pufall, W. H. Rippard, S. E. Russek, S. Kaka, and J. A. Katine, *Phys. Rev. Lett.* **97**, 087206 (2006).
- ²⁰S. Machlup, *J. Appl. Phys.* **25**, 341 (1954).
- ²¹V. Tiberkevich, A. Slavin, and J. V. Kim, *Appl. Phys. Lett.* **91**, 192506 (2007).